



HAL
open science

An Extremely Deep Rubin Survey to Explore the Extended Kuiper Belt and Identify Objects Observable by New Horizons

J J Kavelaars, Marc W Buie, Wesley C Fraser, Lowell Peltier, Susan D Benecchi, Simon B Porter, Anne J Verbiscer, David W Gerdes, Kevin J Napier, Joseph Murtagh, et al.

► **To cite this version:**

J J Kavelaars, Marc W Buie, Wesley C Fraser, Lowell Peltier, Susan D Benecchi, et al.. An Extremely Deep Rubin Survey to Explore the Extended Kuiper Belt and Identify Objects Observable by New Horizons. The Astrophysical Journal Supplement, 2025, 280 (1), pp.8. <10.3847/1538-4365/adea42>. <hal-05226699>

HAL Id: hal-05226699

<https://hal.science/hal-05226699v1>

Submitted on 27 Aug 2025

HAL is a multi-disciplinary open access archive for the deposit and dissemination of scientific research documents, whether they are published or not. The documents may come from teaching and research institutions in France or abroad, or from public or private research centers.

L'archive ouverte pluridisciplinaire **HAL**, est destinée au dépôt et à la diffusion de documents scientifiques de niveau recherche, publiés ou non, émanant des établissements d'enseignement et de recherche français ou étrangers, des laboratoires publics ou privés.



HAL Authorization



An Extremely Deep Rubin Survey to Explore the Extended Kuiper Belt and Identify Objects Observable by New Horizons

J. J. Kavelaars^{1,2,3} , Marc W. Buie⁴ , Wesley C. Fraser^{1,2} , Lowell Peltier^{1,2} , Susan D. Benecchi⁵ , Simon B. Porter⁴ , Anne J. Verbiscer^{4,6} , David W. Gerdes^{7,8} , Kevin J. Napier^{7,9,10} , Joseph Murtagh¹¹ , Takashi Ito¹² , Kelsi N. Singer⁴ , S. Alan Stern⁴ , Tsuyoshi Terai¹³ , Fumi Yoshida^{14,15} , Michele T. Bannister¹⁶ , Pedro H. Bernardinelli^{17,24} , Gary M. Bernstein¹⁸ , Colin Orion Chandler^{17,19} , Brett Gladman³ , Lynne Jones^{20,21} , Jean-Marc Petit²² , Megan E. Schwamb¹¹ , Pontus C. Brandt²³ , and Joel W. Parker⁴

¹ National Research Council of Canada, Herzberg Astronomy and Astrophysics Research Centre, 5071 W. Saanich Road, Victoria, BC, V9E 2E7, Canada; JJ.Kavelaars@nrc-cnrc.gc.ca

² Department of Physics and Astronomy, University of Victoria, Elliott Building, 3800 Finnerty Road, Victoria, BC V8P 5C2, Canada

³ Department of Physics & Astronomy, University of British Columbia, 6224 Agricultural Road, Vancouver, BC V6T 1Z1, Canada

⁴ Southwest Research Institute, 1301 Walnut Street, Suite 400, Boulder, CO 80302, USA

⁵ Planetary Science Institute, 1700 East Fort Lowell, Suite 106, Tucson, AZ 85719, USA

⁶ Department of Astronomy, University of Virginia, P.O. Box 400325, Charlottesville, VA 22904-4325, USA

⁷ Department of Physics, University of Michigan, Ann Arbor, MI 48109, USA

⁸ Department of Astronomy, University of Michigan, Ann Arbor, MI 48109, USA

⁹ Michigan Institute for Data Science, University of Michigan, Ann Arbor, MI 48109, USA

¹⁰ Center for Astrophysics | Harvard & Smithsonian, 60 Garden Street, Cambridge, MA 02138, USA

¹¹ Astrophysics Research Centre, School of Mathematics and Physics, Queen's University Belfast, Belfast BT7 1NN, UK

¹² Center for Computational Astrophysics, National Astronomical Observatory of Japan, Osawa 2-21-1, Mitaka, Tokyo, 181-8588, Japan

¹³ Subaru Telescope, National Astronomical Observatory of Japan, 650 North A'ohoku Place, Hilo, HI 96720, USA

¹⁴ University of Occupational and Environmental Health, 1-1 Iseigaoka, Yahata, Kitakyushu 807-8555, Japan

¹⁵ Planetary Exploration Research Center, Chiba Institute of Technology, 2-17-1 Tsudanuma, Narashino, Chiba 275-0016, Japan

¹⁶ School of Physical and Chemical Sciences — Te Kura Matū, University of Canterbury, Private Bag 4800, Christchurch 8140, New Zealand

¹⁷ DiRAC Institute and the Department of Astronomy, University of Washington, Seattle, WA, USA

¹⁸ Department of Physics and Astronomy, University of Pennsylvania, Philadelphia, PA 19104, USA

¹⁹ Department of Astronomy and Planetary Science, Northern Arizona University, PO Box 6010, Flagstaff, AZ 86011, USA

²⁰ Aeroteck, Suite 150, 4321 Still Creek Drive, Burnaby, BC V5C 6S7, Canada

²¹ Rubin Observatory, 950 N. Cherry Avenue, Tucson, AZ 85719, USA

²² Université Marie et Louis Pasteur, CNRS, Institut UTINAM (UMR 6213), OSU Theta F-25000 Besançon, France

²³ Johns Hopkins University Applied Physics Laboratory, 11100 Johns Hopkins Road, Laurel, MD 20723, USA

Received 2025 January 19; revised 2025 June 26; accepted 2025 June 26; published 2025 August 14

Abstract

A proposed Vera C. Rubin Observatory deep-drilling microsurvey of the Kuiper Belt will investigate key properties of the distant solar system. Utilizing 30 hr of Rubin time across six 5 hr visits over 1 yr starting in summer 2026, the survey aims to discover and determine orbits for up to 730 Kuiper Belt objects (KBOs) to an r -magnitude of 27.5. These discoveries will enable precise characterization of the KBO size distribution, critical for understanding planetesimal formation. By aligning the survey field with NASA's New Horizons spacecraft trajectory, the microsurvey will facilitate discoveries for the mission operating in the Kuiper Belt. Modeling based on the Outer Solar System Origin Survey predicts at least 12 distant KBOs observable with the New Horizons LORRI and approximately three objects within 1 au of the spacecraft, allowing higher-resolution observations than Earth-based facilities. LORRI's high-solar-phase-angle monitoring will reveal these objects' surface properties and shapes, potentially identifying contact binaries and orbit-class surface correlations. The survey could identify a KBO suitable for a future spacecraft flyby. The survey's size, depth, and cadence design will deliver transformative measurements of the Kuiper Belt's size distribution and rotational properties across distance, size, and orbital class. The high stellar density in the survey field also offers synergies with transiting exoplanet studies.

Unified Astronomy Thesaurus concepts: [Kuiper Belt \(893\)](#); [Sky surveys \(1464\)](#)

1. Introduction

The Vera C. Rubin Observatory is nearing operations with the recently completed commissioning camera run. At the time of writing, the Legacy Survey of Space and Time (LSST) will

soon be underway with Rubin first light scheduled for the summer of 2025.²⁵ When operational with LSSTCam, the 8.36 m Simonyi Survey Telescope will image a 9.6 deg² circular field of view (FOV) with a 30 s cadence, alternating between u , g , r , i , z , and y bands. This special issue presents several cadence scenarios developed during the LSST's planning phases, a critical step toward understanding the optimal operations of this multiyear survey. The currently planned cadence for LSST (see F. Bianco & F. The Rubin

²⁴ DiRAC Postdoctoral Fellow.

²⁵ <https://www.lsst.org/about/project-status>

Observatory Survey Cadence Optimization Committee 2024) will enable the discovery of an unprecedented number of small solar system bodies, including trans-Neptunian objects (TNOs), determining precise orbits and physical properties for many more such bodies than are currently known. Rubin will genuinely transform our knowledge of the solar system.

As the start of the LSST nears, the details of how Rubin Observatory will operate are becoming apparent, and there now exists the possibility that the facility’s scheduling budget may accommodate a set of “microsurveys” (consuming more than 10 hr but less than 100 hr) (F. B. Bianco et al. 2022; F. Bianco & F. The Rubin Observatory Survey Cadence Optimization Committee 2023, 2024). For example, time gained by moving from doublets of 15 s exposures to single 30 s exposures, one-snap mode, could provide many 100s of hours for microsurveys.

At the same time, the solar system research community has a second unique opportunity. NASA’s New Horizons mission was specifically designed to characterize bodies in the Kuiper Belt and has made critical, unique contributions, including: (1) Understanding the Pluto–Charon system at an unprecedented level (e.g., S. Desch & M. Neveu 2017; M. L. Wong et al. 2017; S. A. Stern et al. 2015, 2019; V. A. Krasnopolsky 2020). (2) Transforming our understanding of small Kuiper Belt objects (KBOs; S. A. Stern et al. 2019) yielding new constraints on chemistry (W. M. Grundy et al. 2020), cratering and KBO size distributions (K. N. Singer et al. 2019; S. J. Robbins & K. N. Singer 2021), and processes associated with planetesimal accretion (e.g., S. A. Stern et al. 2019, 2023; W. B. McKinnon et al. 2020; D. Nesvorný et al. 2021, 2022, 2023a, 2023b). (3) Enabling studies of small KBO properties (shapes, close satellites, surface characteristics) in ways not otherwise achievable (S. B. Porter et al. 2016; A. J. Verbiscer et al. 2019, 2022).

The spacecraft, currently ~ 61 au from the Sun, continues to be healthy as it moves through the distant Kuiper Belt at a rate of ~ 3 au yr $^{-1}$ for another ~ 15 yr. Like all missions, New Horizons has answered many science questions and raised others. Although the probability of finding a suitable target is low, the close flyby of a more distant KBO, some 2–3 times further from the Sun than Arrokoth, would be an unprecedented and extraordinary scientific and exploration opportunity. Depending on the orbit, these objects could provide in situ measurement of a surface that has experienced a different thermal history than experienced by either Pluto or Arrokoth, thus providing a revolutionary perspective on the evolution of these otherwise inaccessible bodies. New Horizons is the only spacecraft currently operating in the Kuiper Belt, providing a once-in-a-generation opportunity to observe distant KBOs up close.

Here, we consider the opportunity to use a deep-drilling cadence to conduct a Rubin microsurvey to transform our understanding of the Kuiper Belt and find new targets for New Horizons to observe: the New Horizons Deep Drilling Field (NHDDF). This white paper builds on the deep-drilling field for solar system science described in D. E. Trilling et al. (2018), utilizing recent Rubin calibration and operational information, focusing on coordination on the NHDDF, and using recent population models developed by the Outer Solar System Origins Survey (OSSOS; M. T. Bannister et al. 2018). The currently planned Rubin deep-drilling fields²⁶ do not

provide any significant possibility for KBO discoveries as they occur at high ecliptic latitude where the sky density of KBOs is very low. The field closest to the ecliptic plane, COSMOS, at 8° ecliptic latitude, will be blind to the cold classical Kuiper Belt, a population critical to understanding planetesimal formation. The proposed observing cadence is to stare at a single LSST pointing for the maximum low-air-mass time available in the NHDDF, namely ~ 5 hr, on 6 nights/visits to secure orbits and basic classification of the detected sample. Such a project would deliver both unique science on its own and enable the exploitation of New Horizons’ unique capability to observe from within the Kuiper Belt while providing a chance to find a new distant encounter target for the spacecraft to explore. Independent of this opportunity, this microsurvey will illuminate fundamental details of this region of space that have never been feasible to investigate and complement the LSST goals.

2. Deep Drilling in the Solar System with Rubin

Wide-area ground-based TNO surveys have systematically reached a depth of $r \simeq 26.5$ (see W. C. Fraser et al. 2024a; K. J. Napier et al. 2024; F. Yoshida et al. 2024, for recent examples). These surveys use digital tracking techniques, often combined with machine learning–based image recognition, to “shift-and-stack” multiple short exposures. In particular, W. C. Fraser et al. (2024a) utilizes the `kbmod` (H. Smotherman et al. 2021) routine, which was specifically developed to operate on images processed through the Rubin LSST Science Pipeline. W. C. Fraser et al. (2024a) conducted their search in the sky location that is coincident with the New Horizons trajectory. They have demonstrated the ability to achieve near-photon-noise-limit depths on full stacks of digitally tracked images. As outlined in Section 3, a single field Rubin microsurvey using modern digital tracking should achieve a depth of $r \sim 27.5$, the deepest ground-based KBO survey to date, discovering over 700 new KBOs. New search techniques that enable multnight stacking (such as reported by K. Napier 2024) could extend the limit of detection even further, perhaps as deep as $r \simeq 28.2$. Even at slightly shallower depths, Rubin will significantly benefit New Horizons, studies of the Kuiper Belt, and studies of other solar system bodies. Figure 1 presents a view of the currently available, ongoing, or planned KBO surveys; this Rubin microsurvey would probe new depths and provide the significant populations needed to enable new science.

2.1. Kuiper Belt Science

The Rubin Observatory LSST camera’s wide FOV, combined with expected deep-drilling depths, enables the characterization of a deep, extended Kuiper Belt in detail for the first time. Current ground-based detections of distant KBOs, see Figure 2 (W. C. Fraser et al. 2024b; F. Yoshida et al. 2024), as well as measurements by the New Horizons Venetia Burney Student Dust Counter (SDC; A. Doner et al. 2024), give evidence for a potentially sizable component to the disk further out. The >700 KBOs (Table 1) that this proposed 30 hr observation program (5 hr per visit over six visits spanning two oppositions) of the NHDDF will detect include a significant fraction of small objects with $H < 11$ (or smaller,

²⁶ <https://survey-strategy.lsst.io/baseline/ddf.html>

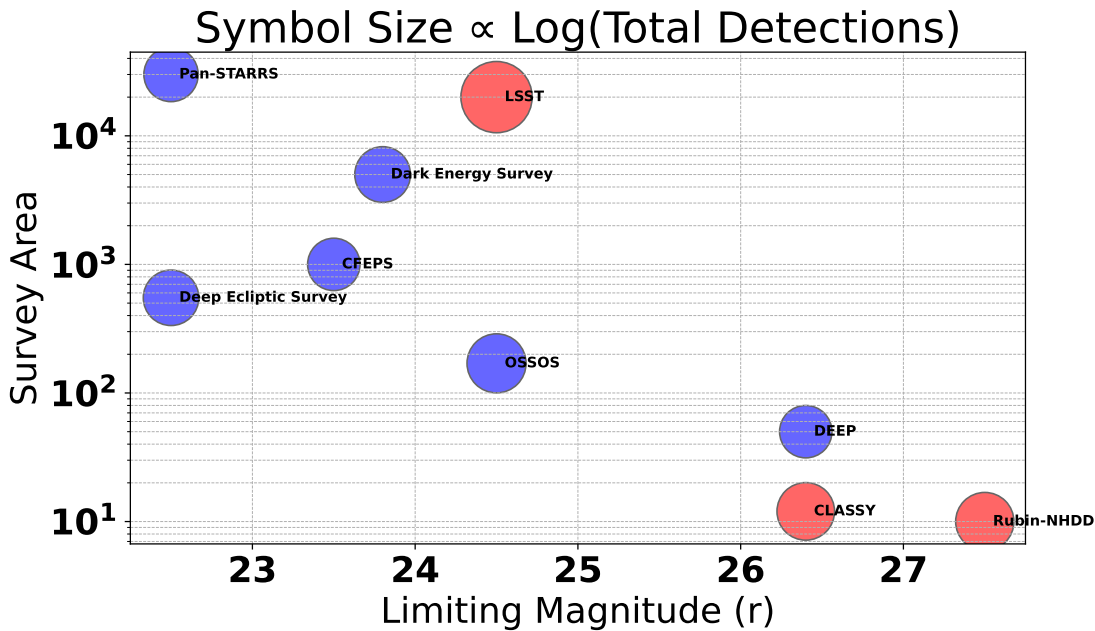


Figure 1. Coverage and depth from various published (blue) and ongoing or planned (red) TNO surveys. The proposed project (Rubin-NHDDF) would reach deeper into the KBO population, opening a new component of this phase space.

dependent on cumulative observing time and sky conditions, see Section 3 for details). These small objects probe a region of the size distribution, see Figure 3, which has been historically limited to space-based telescopes, which come at an exceedingly high observing cost despite the woefully tiny FOVs. Figure 4 shows the probability function versus discovery distance from New Horizons for Rubin discoveries with projected magnitudes of $V < 20.5$ in the spacecraft’s LORRI (A. F. Cheng et al. 2008; H. A. Weaver et al. 2020). A New Horizons close-flyby target would need to be discovered within about 0.03 au of the spacecraft’s current trajectory. Determining the precise likelihood of a flyby is contingent on a more secure determination of the population of the extended Kuiper Belt.

2.2. New Horizons Science

At 61 au, New Horizons is uniquely positioned to explore KBOs in the outer solar system. Owing to the size of the Earth’s orbit, objects beyond Neptune are only visible at solar phase angles (Sun–KBO–observer) $< 2^\circ$ from Earth-based observatories. Observations at larger phase angles are only accessible to spacecraft far from Earth, and New Horizons is the only spacecraft planned to fly between 61 and 106 au for decades. New Horizons LORRI has already observed about three dozen KBOs at high phase angles, characterizing their surface scattering properties, shapes, rotation poles, and periods (S. B. Porter et al. 2016; A. J. Verbiscer et al. 2019, 2022). By applying photometric models to disk-integrated solar phase curves of KBOs, New Horizons has already found correlations between phase function and surface composition (A. J. Verbiscer et al. 2022). KBOs with highly volatile ices on their surfaces have shallower phase curves than those without volatiles, like Arrokoth. These high-phase-angle observations provide insight into object composition and, by inference, its formation location. Six of these objects were observed when closer than 1 au to the spacecraft; one was

found to be a tight binary on a presumably circular orbit, another a contact binary, and a third very likely a binary (H. A. Weaver et al. 2022). Rotation light curves acquired at multiple high phase angles have also revealed a high fraction of contact binaries (S. Porter et al. 2024), suggesting that more than 50% of the small KBO population are in multiple or contact systems. The closeness of these binary pairs and pole projections of the contact systems required the resolution and/or viewing geometry of LORRI to be revealed. Since New Horizons has left the densely populated classical Kuiper Belt, the KBOs that this Rubin microsurvey would find for study with LORRI are members of more distant populations, some with apoapses that extend beyond the heliopause. Modeling based on the known Kuiper Belt indicates that LORRI would be able to view the ~ 3 targets within 1 au, providing high spatial resolution for tight satellite discoveries and nine additional targets at a longer range.

2.3. The Distant Kuiper Belt

At the time of writing, numerous ultradeep surveys are ongoing. The main goals of these surveys are to measure the size distribution of Kuiper Belt populations down to much smaller sizes and with significantly higher fidelity than previously done (e.g., H. Smotherman et al. 2024, see S. M. Lawler & R. E. Pike 2024 for a recent summary). One of the surprising results coming from some of these surveys is the potential discovery of a heretofore unrecognized massive population of distant bodies. Observations presented by W. C. Fraser et al. (2024a) imply distant regions that were previously thought to be relatively empty have a factor of ~ 4 more objects at a distance $r \gtrsim 70$ au than detected in previous surveys (M. T. Bannister et al. 2018). Such a population would rival the most massive subpopulations of more proximate KBO populations, such as the population of 3:2 mean-motion resonators, and would represent a significant increase in the bounds of what was previously considered the outer bound of

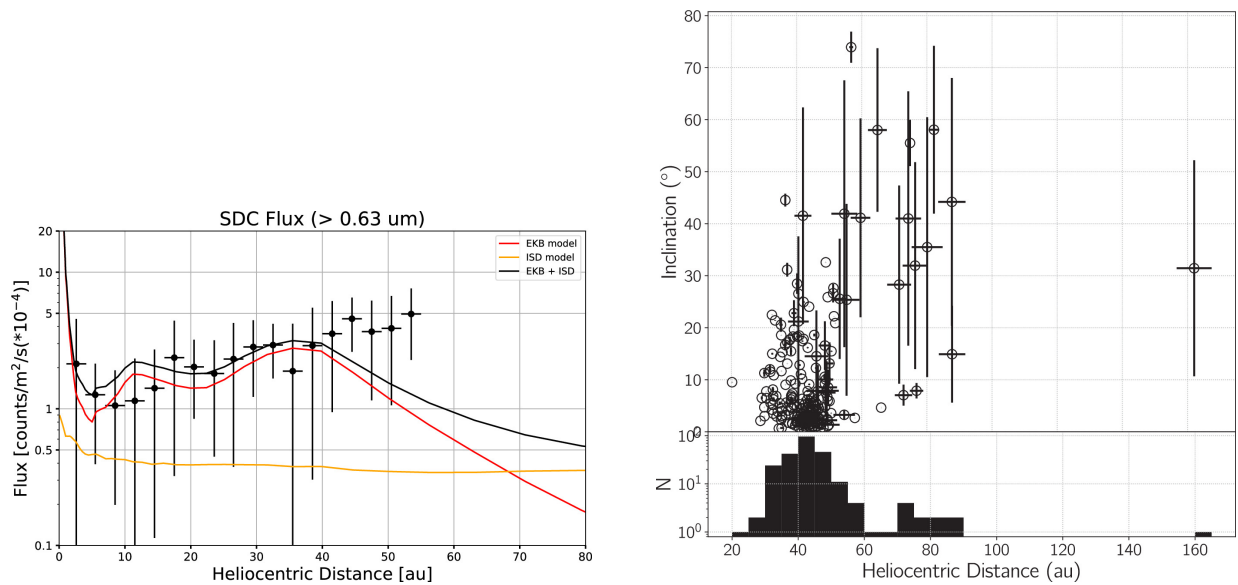


Figure 2. (Left) Figure 3 from A. Doner et al. (2024, used with permission), showing SDC flux estimates for particles with a radius greater than $0.63 \mu\text{m}$ from 1 to 55 heliocentric astronomical units. Each point averages the flux measured by each film across each 3 au traversed by the New Horizons spacecraft. (Right) Figure 1 from W. C. Fraser et al. (2024b, used with permission), showing the inclination and distance of the New Horizons discoveries from Subaru Telescope Hyper Suprime-Cam observations 2020–2023. A histogram of the heliocentric distances is shown in the bottom panel, with a bin width of 5 au chosen to be similar to the typical uncertainty of the objects with best-fit heliocentric distance $R > 70$ au. These data suggest that many KBOs are located ahead of New Horizons and may be accessible to it for observation.

Table 1

Expected KBO Discoveries from the New Horizons Deep-drilling Field

Search Depth r (5σ)	No. Obs.		Total No.	Rubin Time (hr) ^a
	No. <1 au	by NH		
27.0	1.2	6	450	12
27.5	2.9	12	780	30
28.0	4.6	22	1280	75
28.5	7.6	38	2000	180

Note.

^a Total time required to enable discovery and first-order orbit determination, six visits over one year.

the known Kuiper Belt (~ 55 au; referred to as the Kuiper cliff). Such objects could even be the start of the Kuiper wall, representing a rebound in the primordial surface density of the Sun’s protoplanetary disk (E. I. Chiang & M. E. Brown 1999). A putative Kuiper wall could have escaped detection under the assumption that such a distant population may have formed with a truncated size distribution that, as did the cold classical Kuiper Belt, and is devoid of objects with $H_r \lesssim 5$ (B. Gladman & K. Volk 2021; L. Peltier et al. 2022). Wide-area surveys would need to have reached depths of $r < 24.5$ to have found the very largest objects, of which there would be only a few in such a population.

Fundamentally, this Rubin microsurvey will elucidate the distant regions beyond the main Kuiper Belt in ways otherwise currently unobtainable (J. Kavelaars et al. 2020). At 70 au objects with $r = 27$ have $H_r \sim 8.5$. If the size–frequency distribution of the distant bodies follows the slope typical for KBOs in a similar size range ($N(H) \propto 10^{\alpha H}$, $\alpha \sim 0.6$), then the sky density of these distant objects at magnitude $r \simeq 27.5$ will be roughly 4 times higher than at the current state-of-the-art Subaru depths ($r < 26.5$). As such, considering the Rubin areal coverage and depth, we would expect ~ 80 newly detected

objects at and beyond 70 au. (W. C. Fraser et al. (2024a) reported 11 in 5 deg^2 compared to Rubin’s 11 deg^2 FOV.) Given the wide range of distant Kuiper Belt population estimates, the chance this survey could find an encounter target for New Horizons is difficult to assess without more precise knowledge of this putative distant population. Should this distant population be confirmed, the chance of finding an encounter target is significantly enhanced. However, this enhanced distant population is only putatively detected, and its orbital distribution is unknown. Predicting the encounter probability based on this imprecise knowledge is premature. This Rubin microsurvey would confirm this distant population, enable its first direct characterization, and provide the tracking observations needed to ensure a high level of veracity to the detections of these distant bodies to confirm the previously reported overdensity, compared to the OSSOS++ model (J.-M. Petit et al. 2023a).²⁷

If these distant KBO origins are with the dynamically excited KBOs, then one would expect them to have moderate to high inclinations and eccentricities, and their orbits would be coupled to Neptune. Objects in resonance with Neptune come to their apocenters in the area searched by W. C. Fraser et al. (2024a) and could be an explanation for their detections. If these distant objects formed from a cold disk and were pushed out during smooth migration, they would be found with low inclinations and moderate eccentricities, still dynamically coupled to Neptune, or, if they are from a second Kuiper Belt, they would be entirely uncoupled from Neptune. Current data poorly constrain the orbital distribution of the distant objects reported by W. C. Fraser et al. (2024a). In these circular orbit cases, one might expect a truncated size distribution to have

²⁷ The OSSOS++ Kuiper Belt model assembles the classical Kuiper Belt, resonant, scattering, and detached populations described in a series of papers from the OSSOS group: M. T. Bannister et al. (2018), S. M. Lawler et al. (2018), J. J. Kavelaars et al. (2021), B. L. Croomvoets et al. (2022), J.-M. Petit et al. (2023b), and M. Beaudoin et al. (2023).

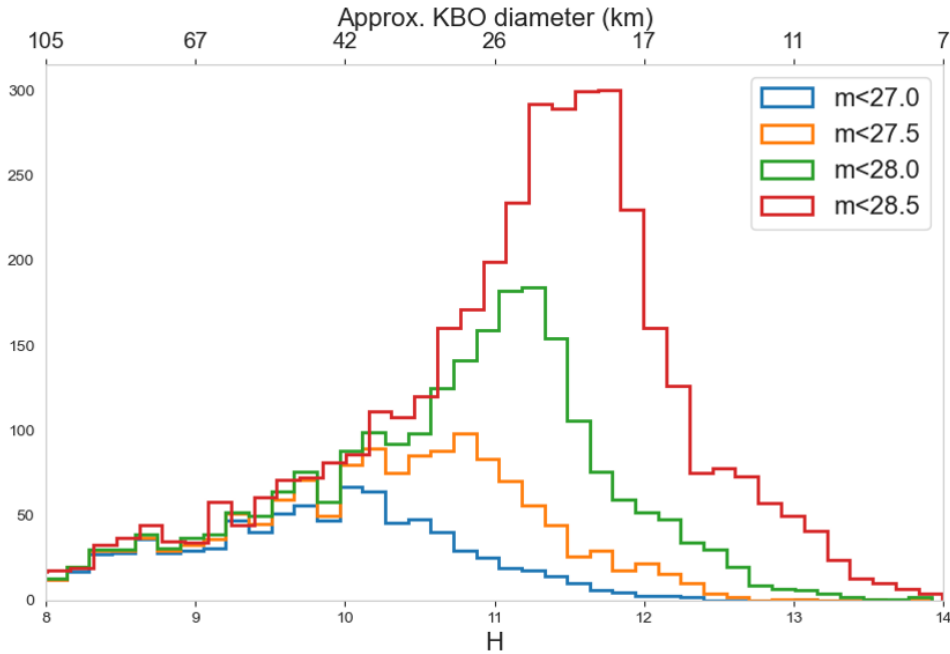


Figure 3. H magnitude distribution for KBOs discoverable at the New Horizons search location as a function of survey depth. The input model is the OSSOS++ model and does not include the putative distant population; see text for details. The corresponding size of these objects, assuming an albedo of $p_V = 0.10$, is shown along the top axis. The y-axis is the number of objects discovered at each H magnitude/size based on survey magnitude depth, denoted by the color shown in the inset key.

hidden them from the view of wide-area surveys with limits of <24.5 .

2.4. Size Distribution, KBO Formation, and Cratering

Through the brightness range $r < 26$, where the sample of KBOs has been measured robustly, we see a size distribution that is compatible with expectations from modern planetesimal growth models, such as the streaming instability (J. J. Kavelaars et al. 2021; J.-M. Petit et al. 2023b; K. J. Napier et al. 2024). Available surveys demonstrate that the number-density distribution of objects smaller than ~ 400 km diameter, through the observable range, results in a uniform total mass per unit size. As such, observations of objects in this size range provide limited leverage on protoplanetary disk models. Only at the faint end of what is reachable from current telescope offerings does the distribution exhibit deviations away from equal mass per size bin (K. J. Napier et al. 2024). These deviations are critical in elucidating the formative processes outer solar system objects have experienced, but available measurements come with extremely poor fidelity simply due to the low numbers of small KBOs detected to date; at the time of writing, only ~ 10 KBOs fainter than $r = 26.5$ have ever been detected with robust orbit determination (G. M. Bernstein et al. 2004; H. Smotherman et al. 2024). Simulations of macroscopic bodies formed via streaming instability predict that below a specific size, objects are no longer the primary accretion products of pebble-cloud collapse but rather are the unaccreted detritus that is ejected during collapse (e.g., J. E. Robinson et al. 2020; B. Polak & H. Klahr 2023). Probing this process requires reaching sizes below those produced by pebble-cloud collapse, providing evidence for how collisionally evolved this small-sized material is, how high the collisional interactions during accretion were, and what the accretion efficiency (mass ratio of detritus to

macroscopic bodies) is. All of these are fundamental to understanding planetesimal growth and currently remain out of reach, at least until this microsurvey is executed.

There are no known plans to conduct surveys that go both broad and deep enough that they can directly connect the large ($D > 200$ km) object slope and small ($D < 20$ km) object slopes to provide a robust measure of the preferred size scale of the Kuiper Belt’s planetesimal population. This Rubin microsurvey will provide a sample of KBOs that vastly improve upon the known faint sample while simultaneously directly connecting to the bright object distribution (~ 10 objects with $r < 23.3$ will be in the FOV). A survey to $r < 27.5$ will provide a sample of $\lesssim 730$ discoveries, with the majority being fainter/smaller than where the fidelity of the known sample crumbles. The discovered sample will increase by a factor of $\sim 2\times$ for every ~ 0.5 mag increase in depth limit.

2.5. Rotational Light Curves

The planned survey cadence will also provide an exceptional measure of the rotational properties of the KBOs, another indicator of the planetesimal formation process. Exposures for each of the six visits will be 30 s, resulting in 540 exposures per 4.5 hr of integration (taking 5 hr with overheads) at each visit. The NHDDF field is included in the planned coverage of LSST. Based on the recent operational simulations (one_snap_v3.6_10yrs.db; doi:10.11570/25.0091) this field will be visited ~ 100 times per filter throughout the survey. Based on simulations using one_snap_v3.6_10yrs.db, the OSSOS++ model, and *Sorcha* (see Section 3 for details), we expect the LSST project will provide an orbital classification for the ~ 30 KBOs within the NHDDF. For this sample of objects, the deep sampling provided by the NHDDF fields will enable detailed studies of the rotational state of the objects. This information can be used to further explore the

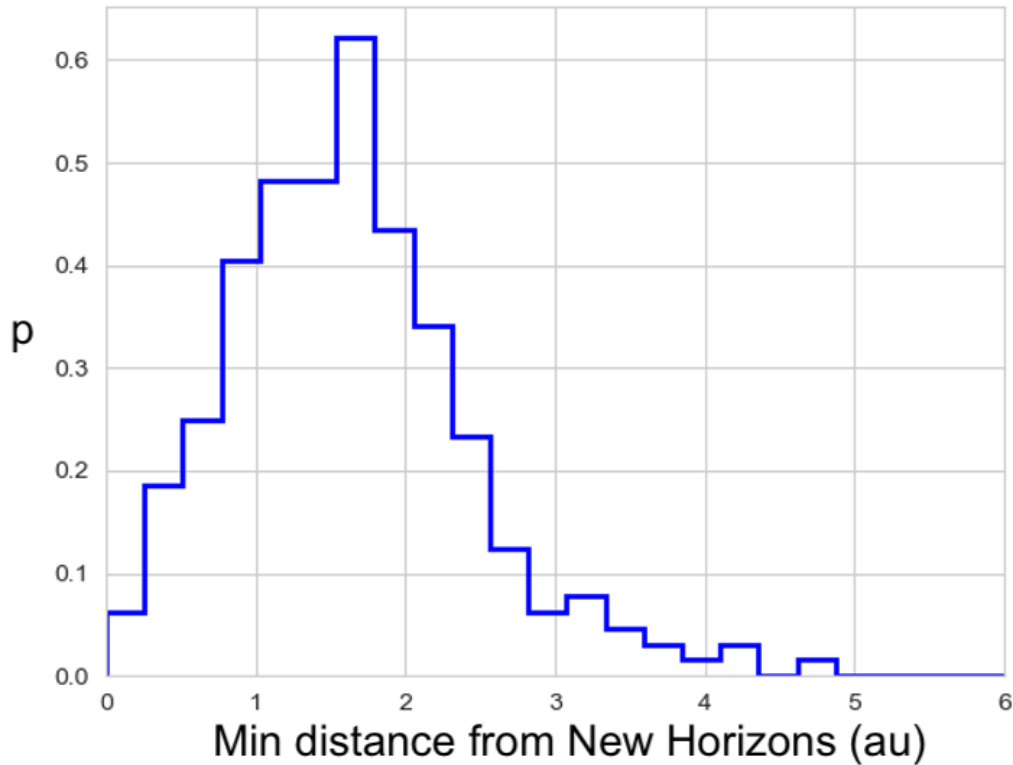


Figure 4. The probability density (p) vs. discovery distance from the New Horizons spacecraft for Rubin discoveries with projected LORRI magnitudes of $V < 20.5$ and currently beyond 70 au. Approximately 40% of objects discovered beyond 70 au will come within 1 au of the spacecraft.

relationship between object shape and size, an indicator of collisional evolution processes in the outer solar system (S. D. Benecchi & S. S. Sheppard 2013).

In addition to this, combining data across and within visits will enable the determination of light-curve amplitudes for much fainter sources (see R. Strauss et al. 2024, for example) and will provide bulk-shape information. A rolling window through the full time series will allow likelihood-based measurements of the amplitudes of light curves for these faint objects. For example, measurement at 10σ of 26th magnitude sources requires approximately 150 exposures (based on the 5σ limit of 27.5 in 540 exposures). Each visit will provide four independent time windows during which sources as faint as 26th magnitude can be measured at 10σ . The expectation is to achieve six visits to the field, resulting in 24 (6×4) independent flux measurements. If the timing of the mid-observation for each visit is shifted by 1 hr per night, and the observations taken weeks and months later are further shifted in time, this will remove the 12 and 24 hr aliases from this coarse sampling of these faint light curves. The 24 samples of about 1.25 hr duration each will provide the rotation amplitudes, and thus bulk-shape information, for 100 KBOs.

2.6. Occultation Opportunities

Near Galactic coordinates $l = 17.5$, $b = -14.8$, the NHDDF is near the Galactic center and has a high stellar density (see Figure 5). Although challenging, previous searches (e.g., W. C. Fraser et al. 2024a) have demonstrated the feasibility of difference imaging in this part of the sky, achieving near-photon-noise-limit detections using the LSST Science Pipeline’s differencing engine. At the same time, the high stellar density provides a high likelihood that many newly

discovered objects can have their physical sizes measured via predicted stellar occultations. Among the sample of discovered objects that have occultations, some will be drawn from the ~ 100 KBOs of which we expect to have determined rotational light curves, providing the opportunity to link these objects’ light-curve-derived shapes and occultation-measured shapes. Existing occultation facilities (e.g., M. W. Buie & J. M. Keller 2016) and teams will pursue many of these opportunities. Occultation-based shape measurements will provide a solid link between the physical shapes of these KBOs and their rotational light curves, further enhancing our knowledge of the formation and evolution processes at work in the Kuiper Belt.

3. Solar System Deep-drilling Observing Strategy

3.1. Cadence

This survey aims to detect the faintest moving sources within a microsurvey budget while obtaining sufficient visits to enable moderately precise orbits. Sky motion is a few arcseconds per hour for distant solar system bodies (those beyond 30 au). For such distant bodies, measurements at four epochs in a single observing season, two visits in each of two different lunations, are sufficient to achieve the ephemeris precision needed to enable linking in the following year. In the following year, one must obtain measurements at two epochs to secure the recovery of the object. Given the field location, the opposition observations (two visits) should occur in July, while the two tracking visits would be best scheduled in September. One year later, the recovery should occur over two visits separated by a few nights and taken between May and August of the following year. With these two epochs of observation, one can compute accurate distances and orbital

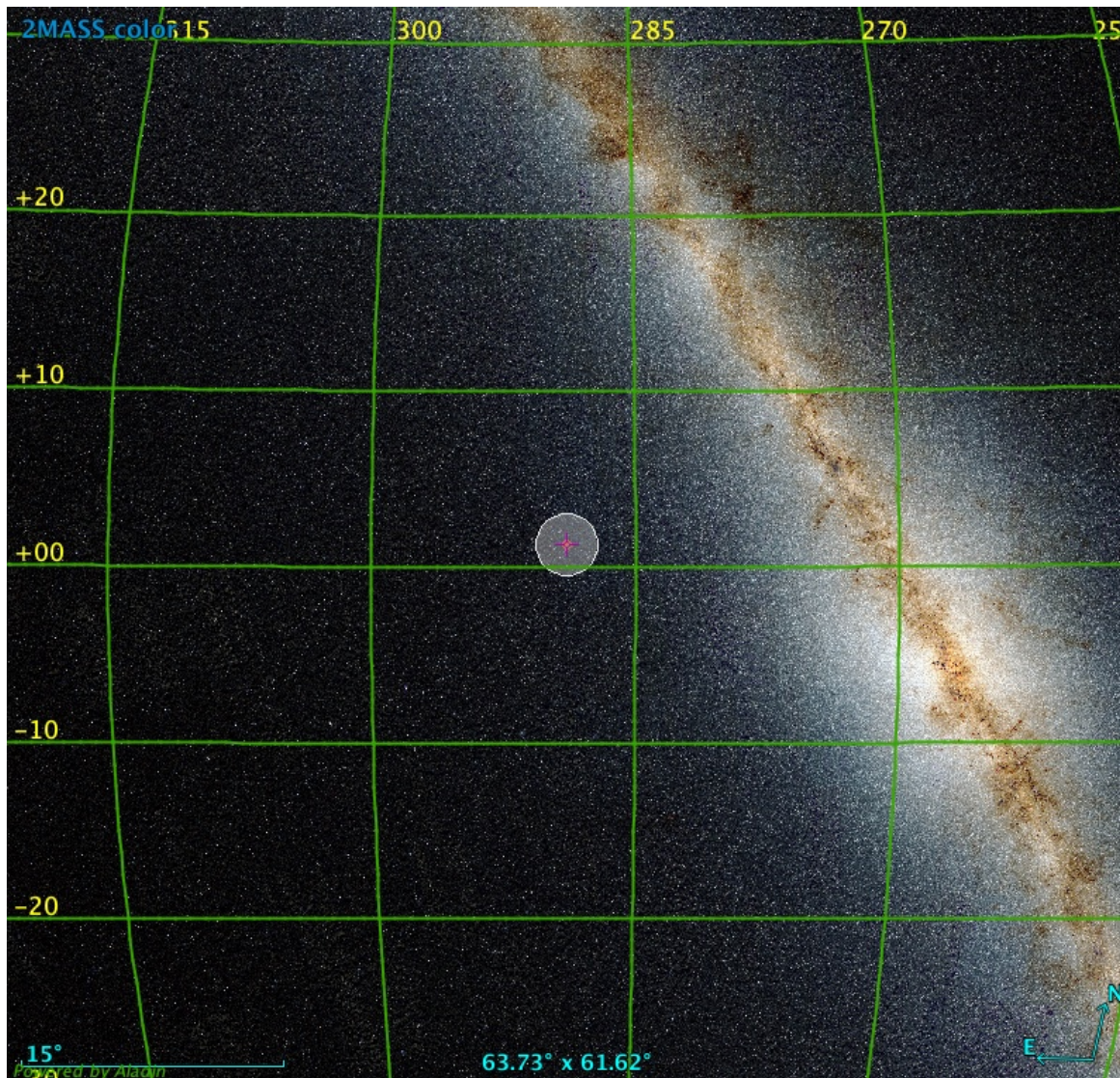


Figure 5. The opaque circle indicates the NHDDF relative to the Galactic plane (image from 2MASS M. F. Skrutskie et al. 2006) displayed using the Aladin Sky Atlas (F. Bonnaire et al. 2000). The coordinate grid is latitude by longitude in ecliptic degrees.

inclinations and have some security in the determination of the semimajor axis of the orbit (see, for example, Figure 10 in M. T. Bannister et al. 2016). This information is sufficient to determine the size distribution, particularly to separate objects into the two main KBO orbital groups of “cold” and “excited” orbits. Those objects found beyond 70 au, of which the OSSOS++ model predicts as many as ~ 40 , can be pursued using large-aperture and space-based facilities with smaller FOVs but greater sensitivity (e.g., Hubble Space Telescope, JWST, Gemini, Magellan). Visits consisting of 5 hr integrations would allow for the six needed visits within the expected 30 hr limit for microsurveys.

3.2. Depth

Given the interplay between object reflectivity and solar flux and the desire to achieve the faintest (small and or distant) detections possible within the time constraints, the survey observations will be obtained in a single Rubin filter, r . A depth of $r \sim 27.5$ can be achieved in each of the six visits to a single Rubin FOV with a 30 hr investment of observing time.

For the moving-source discovery and tracking cadence proposed here, we limit our total exposures to be within a single night and when the field is above an air mass of 1.5, providing ~ 4.5 hr of exposure time per night both when the field is at opposition and 8 weeks later when the field would be reobserved to enable recovery observations of sources detected during opposition. Utilizing the latest throughput information expressed in `rubin_scheduler.utils.m5_scale`,²⁸ sky brightness from the ESO Sky Model,²⁹ an average air mass of 1.3 and 540 30 s exposures predicts a stack depth of $m_r \sim 27.5$. A solar system object survey to this depth over this area of sky with built-in tracking will be unprecedented.

3.3. Field Selection

To enable detection of sources that can be observed from New Horizons requires observing the field near R.A. = 289.4,

²⁸ <https://rubin-scheduler.lsst.io/>

²⁹ <https://www.eso.org/observing/etc/bin/gen/form?INS.MODE=swspectr+INS.NAME=SKYCALC>

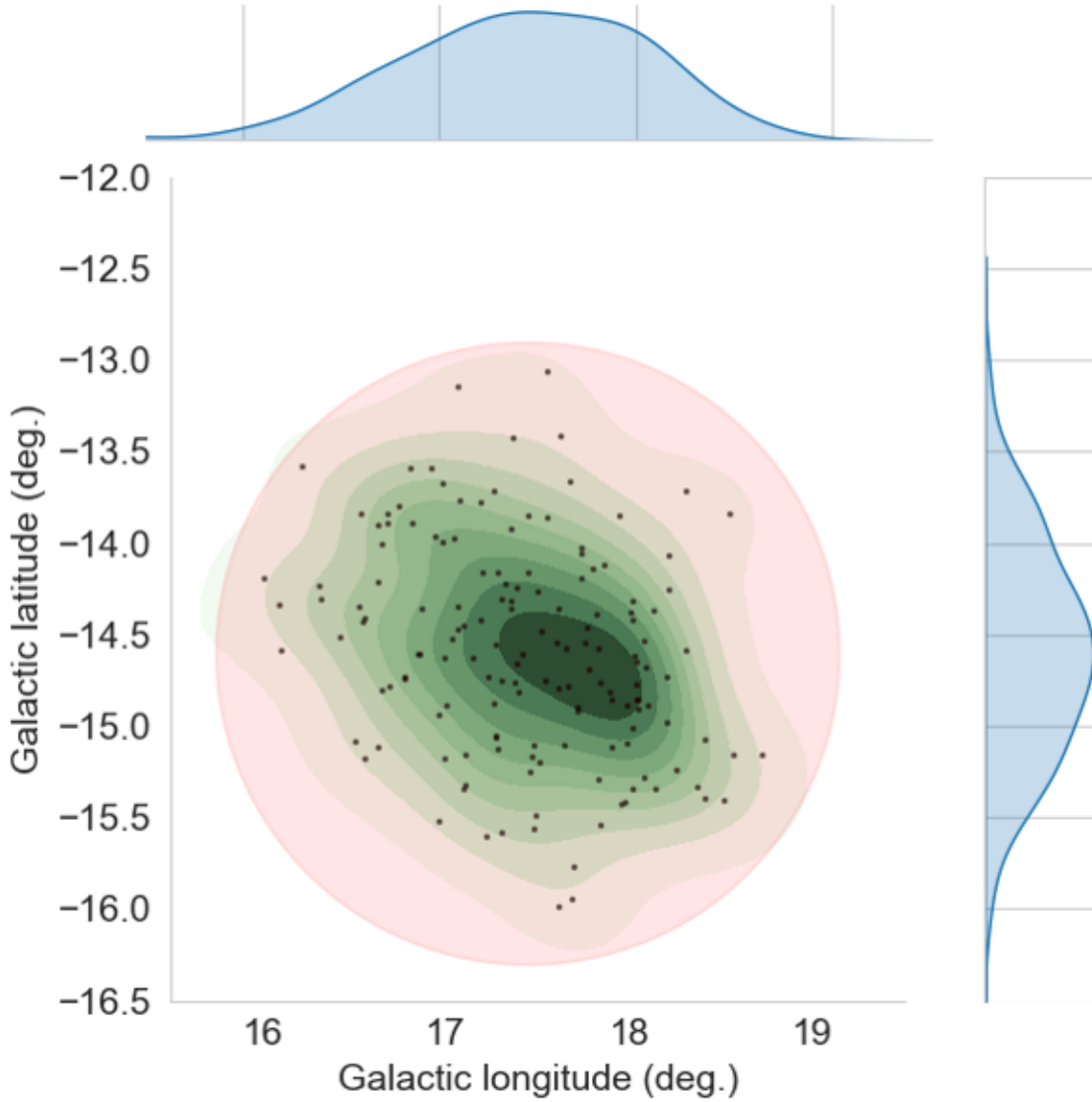


Figure 6. New Horizons search field with the Rubin footprint (pink circle). This plot shows the current sky locations of model objects (black points and sky-density contours) that pass within 1 au of New Horizons between 2027 and 2040 and have $r < 28.5$ in 2026 July. The model is based on the OSSOS++ sample (J.-M. Petit et al. 2023a) and is a $20\times$ oversampling of the expected total population of the Kuiper Belt.

decl. = -20.2 (Figure 5). This field is defined as the search region for objects that are at least 66 au from the Sun between 2027 January 1 and 2040; are within 7° on the sky of New Horizons' location as seen from the Earth in 2026 July (see Figure 6); will pass within 1 au of New Horizons before 2040; and will have $r < 28.5$ in 2026 July. Model orbits are drawn from the OSSOS++ Kuiper Belt model.

Previous surveys at this longitude have revealed an overdensity of sources, while deep surveys at other longitudes (e.g., K. J. Napier et al. 2024) have not reported an overdensity of distant objects. This result may indicate that the W. C. Fraser et al. (2024a) detections are Neptune-resonant objects coming to apocenter at this longitude; the Rubin-NHDDF survey will reveal if this is the case.

In addition to providing targets for LORRI, the high stellar density in this field enables the occultation science case and the possibility of conducting parallel surveys for variable stars and transiting planets near the disk of the Milky Way.

3.4. Expected Detections

We used the 1.0b release of the *Sorcha* (M. J. Holman et al. 2025; S. R. Merritt et al. 2025) package to simulate the impact of our cadence, total integration time, and field choice on the number of KBOs detected. *Sorcha* computes the ephemeris of the objects, given an orbit input file, and determines if the object lands on the footprint of LSSTCam, given a database of pointings. For sources on the footprint, *Sorcha* determines the flux, including sky and shot noise, Rubin would measure in the r filter using an assigned H value, the ephemeris, and the phase angle of the observation. (We used *Sorcha*'s HG phase model with a slope of 0.15.) To ensure that *Sorcha* did not model in trailing losses we modeled the NHDDF observations as a series of visits to a single Rubin pointing where each visit consisted of a single 30 s exposure whose 5σ limit was varied between 27 and 28.5 in r using *Sorcha*'s fading function to express the shape of the detection efficiency curve, setting the width to 0.15 and peak detection efficiency to 0.85 (to account for some area loss

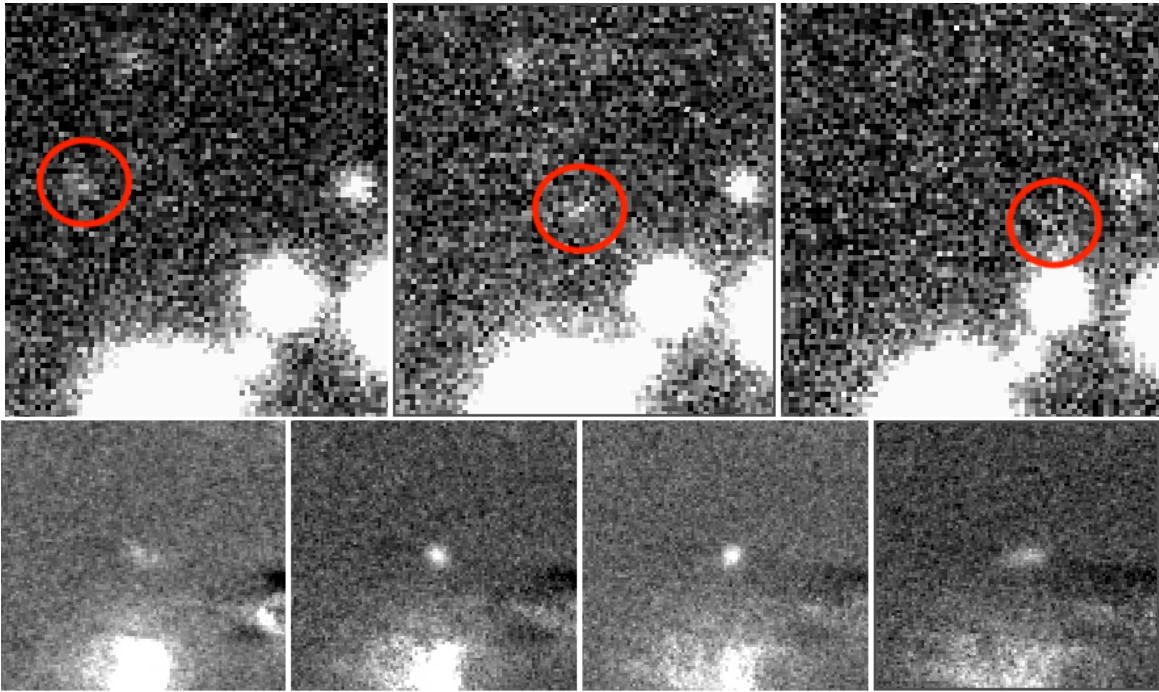


Figure 7. Example of detection of a real moving object made via the shift-and-stack technique from W. C. Fraser et al. (2024a). Top: three individual frames acquired with the Hyper Suprime-Cam on the Subaru Telescope. Red circles mark the object’s positions, barely visible above the noise floor. Bottom: shift-stacks of difference imagery from the same regions as presented above. The stacks were made at rates of motion of 0.5 , 1.0 , 1.5 , and 2.0 hr^{-1} (left to right). The true rate of motion of the object is 1.9 hr^{-1} .

due to nearby bright stars). The short 30 s exposure used to simulate our full stack depth ensured no trailing losses (which *Sorcha* simulates). In the real survey, the detection is conducted using a shift-and-stack process on the 540 30 s exposures on a grid that mitigates trailing loss. The six visits were spaced with two near opposition, two about 8 weeks later, and two about 1 yr later. Each visit was assigned an image quality of $0.8''$, typical of expectations for Rubin. The *Sorcha* tracklet-linking step was not used. Instead, we collated the object and field ID values to determine which model objects were detected in each visit. We ran 20 realizations of the OSSOS++ model for each flux limit. Based on these simulations (see Table 1), we find the NHDDF would result in the detection of 780 ± 50 KBOs, and the offset strategy, trailing the field at the mean motion of all sources beyond 50 au, results in $\sim 94\%$ of all KBOs in the model being recovered in the second opposition.

Based on these simulations, we expect the survey to discover ~ 12 KBOs observable by LORRI, of which ~ 3 will approach within 1 au of New Horizons. Table 1 shows the number of KBOs projected to be within 1 au of the spacecraft for different survey depths. Estimates provided here are based on the OSSOS++ model and do not include the putative distant population reported in W. C. Fraser et al. (2024a); including that population would double or quadruple the distant detections. A search to $m = 28.5$ would require a total of 200 hr. Nevertheless, even a microsurvey of 30 hr on the New Horizons field proposed here yields a significant possibility for objects accessible for observations from the spacecraft. If the enhanced population reported in W. C. Fraser et al. (2024a), which we have not used in our detection estimate here, proves correct, the number of targets seen within 1 au will be a factor of ~ 4 higher. While the probability of one of those targets being a flyby candidate is low, it is not zero.

3.5. Scheduling

As New Horizons moves farther through the belt, the opportunity for observations and encounters diminishes, making discovery and follow-up urgent. For all objects that could potentially be targeted by New Horizons or that are sufficiently scientifically interesting, we will propose follow-up observations with JWST and/or HST to provide additional astrometry to refine their orbits and measure their broadband colors. In 2020, the New Horizons project demonstrated this process with KBO targets discovered by Subaru in June–July, recovered by Subaru in August–September, recovered with HST in November, and then observed by New Horizons in December. A similar timeline for objects discovered in the 2026 July–August or 2027 oppositions by a Rubin micro-survey would be possible; with rapid follow-up the field passes through the HST field of regard, starting ~ 45 days after opposition and lasting ~ 50 days enabling LORRI observations as early as the spring of 2027 or 2028 (observations with Rubin in early fall 2025 would enable New Horizons follow-up in 2026).

3.6. Analysis Techniques

Because Pluto was traversing the Galactic plane when New Horizons flew past it, most of the search region for spacecraft flyby targets has been in highly populated stellar fields. This Rubin survey must, therefore, also be carried out near the Galactic plane ($b \sim -14.8^\circ$) and at a position along the New Horizons trajectory because it allows both characterization of the deep Kuiper Belt and the potential discovery of one final flyby object for the spacecraft (Figure 5). W. C. Fraser et al. (2024b) and F. Yoshida et al. (2024) have developed shift-and-stack techniques (see Figure 7), which provides nonsidereal stacks of images acquired within a single night for source

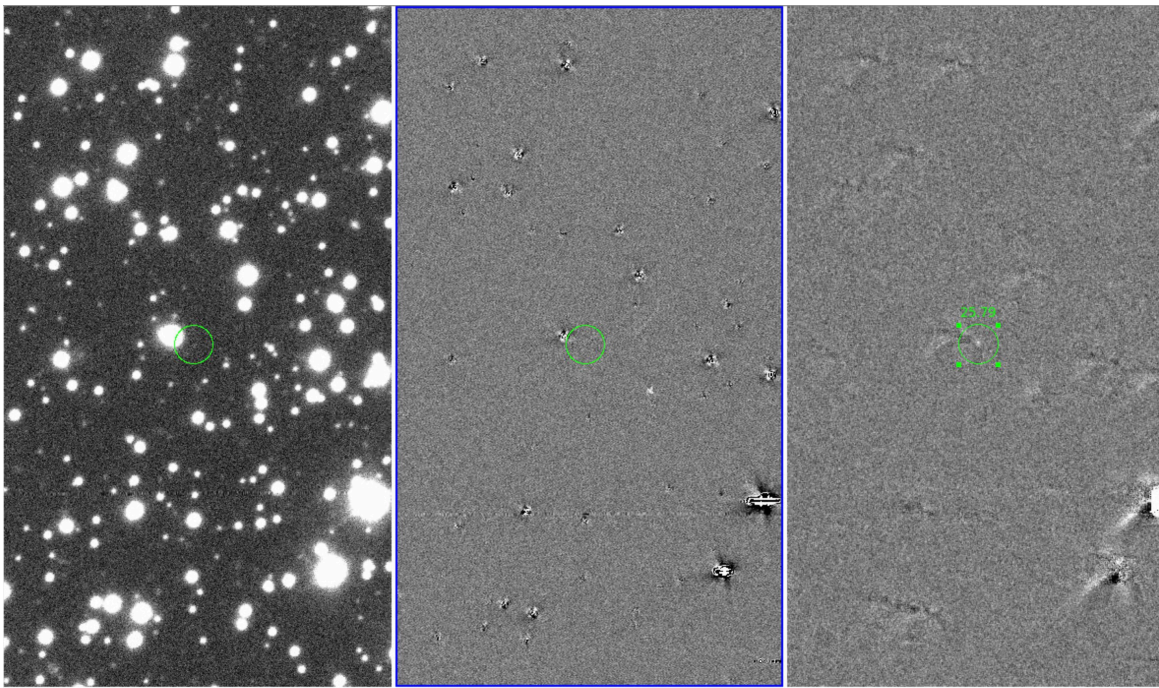


Figure 8. A sample of image-series stacks followed by subtraction of a sky template of stable sources, and then identification of moving objects within those differenced images.

detection and link those source detections on separate nights for validation of detection objects. The technique does not require a separate set of template observations as the reference image used for differencing is built from the microsurvey observations. The field shifts between nights are blind to the detection process (i.e., the detections from one night are not used to plan future fields), and the template is built from the microsurvey observations combined across multiple visits. Over time, highly effective machine learning techniques have also been developed to cope with these dense sky backgrounds and false positives (Figure 8; see also M. W. Buie et al. 2024; W. C. Fraser et al. 2024a; K. J. Napier et al. 2024). These techniques will be applied to search for KBOs in the proposed microsurvey, but they can also be used to search for other small-body populations in the NHDDF.

4. Summary

This white paper proposes an extremely deep Rubin microsurvey in the New Horizons trajectory field (the NHDDF) to both look for spacecraft-accessible KBOs for close flyby or distant study at high-solar-phase angles and possibly at high spatial resolution and to investigate fundamental properties of the distant solar system. As designed, this survey, using 30 hr of Rubin time spread over six 5 hr visits (four spanning two lunations in the first year, two in the following year), will discover and determine orbits for as many as 730 KBOs to a Rubin r magnitude of 27.5, providing a unique opportunity for groundbreaking Kuiper Belt science specifically related to the size distribution. It may discover as many as 12 KBOs observable with the New Horizons LORRI camera and ~ 3 objects within 1 au of the spacecraft. Rapid follow-up of particularly interesting Rubin discoveries with HST or JWST could enable New Horizons observations as early as one year after the discovery opposition visits.






Acknowledgments

We thank NASA for funding and continued support of the New Horizons mission; this work was supported by the New Horizons Project (NASW-02008). This research has made use of NASA’s Astrophysics Data System Bibliographic Services. This research has used data and/or services provided by the International Astronomical Union’s Minor Planet Center. Some of the results in this paper have been derived using the healpy and HEALPix³⁰ packages. This research used the Canadian Advanced Network For Astronomy Research (CANFAR) operated in partnership by the Canadian Astronomy Data Centre and The Digital Research Alliance of Canada with support from the National Research Council of Canada, the Canadian Space Agency, CANARIE, and the Canadian Foundation for Innovation.

Software: Sorcha (M. J. Holman et al. 2025; S. R. Merritt et al. 2025), ASSIST (M. J. Holman et al. 2023; H. Rein et al. 2023), Astropy (Astropy Collaboration et al. 2013, 2018, 2022), Healpy (A. Zonca et al. 2019; K. M. G’orski et al. 2005), Matplotlib (J. D. Hunter 2007), Numba (S. K. Lam et al. 2015), Numpy (C. R. Harris et al. 2020), pandas (W. McKinney 2010; The pandas development team 2020), Pooch (L. Uieda et al. 2020), PyTables (<https://www.pytables.org>), REBOUND (H. Rein & S. F. Liu 2012; H. Rein & D. S. Spiegel 2015), rubin_sim (R. L. Jones et al. 2018; P. Yoachim et al. 2022), sbpy (M. Mommert et al. 2019), SciPy (P. Virtanen et al. 2020), Spiceypy (A. Annex et al. 2020), sqlite (<https://www.sqlite.org/index.html>), sqlite3 (<https://docs.python.org/3/library/sqlite3.html>), tqdm (C. da Costa-Luis et al. 2023), Black (<https://black.readthedocs.io/en/stable/faq.html>), Jupyter Notebooks (T. Kluyver et al. 2016).

³⁰ <http://healpix.sf.net>

ORCID iDs

J. J. Kavelaars  <https://orcid.org/0000-0001-7032-5255>
 Marc W. Buie  <https://orcid.org/0000-0003-0854-745X>
 Wesley C. Fraser  <https://orcid.org/0000-0001-6680-6558>
 Lowell Peltier  <https://orcid.org/0000-0002-9179-8323>
 Susan D. Benecchi  <https://orcid.org/0000-0001-8821-5927>
 Simon B. Porter  <https://orcid.org/0000-0003-0333-6055>
 Anne J. Verbiscer  <https://orcid.org/0000-0002-3323-9304>
 David W. Gerdes  <https://orcid.org/0000-0001-6942-2736>
 Kevin J. Napier  <https://orcid.org/0000-0003-4827-5049>
 Joseph Murtagh  <https://orcid.org/0000-0001-9505-1131>
 Takashi Ito  <https://orcid.org/0000-0002-0549-9002>
 Kelsi N. Singer  <https://orcid.org/0000-0003-3045-8445>
 S. Alan Stern  <https://orcid.org/0000-0001-5018-7537>
 Tsuyoshi Terai  <https://orcid.org/0000-0003-4143-4246>
 Fumi Yoshida  <https://orcid.org/0000-0002-3286-911X>
 Michele T. Bannister  <https://orcid.org/0000-0003-3257-4490>
 Pedro H. Bernardinelli  <https://orcid.org/0000-0003-0743-9422>
 Gary M. Bernstein  <https://orcid.org/0000-0002-8613-8259>
 Colin Orion Chandler  <https://orcid.org/0000-0001-7335-1715>
 Brett Gladman  <https://orcid.org/0000-0002-0283-2260>
 Lynne Jones  <https://orcid.org/0000-0001-5916-0031>
 Jean-Marc Petit  <https://orcid.org/0000-0003-0407-2266>
 Megan E. Schwamb  <https://orcid.org/0000-0003-4365-1455>
 Pontus C. Brandt  <https://orcid.org/0000-0002-4644-0306>
 Joel W. Parker  <https://orcid.org/0000-0002-3672-0603>

References

- Annex, A., Pearson, B., Seignovet, B., et al. 2020, *JOSS*, **5**, 2050
 Astropy Collaboration, Price-Whelan, A. M., Lim, P. L., et al. 2022, *ApJ*, **935**, 167
 Astropy Collaboration, Price-Whelan, A. M., Sipőcz, B. M., et al. 2018, *AJ*, **156**, 123
 Astropy Collaboration, Robitaille, T. P., Tollerud, E. J., et al. 2013, *A&A*, **558**, A33
 Bannister, M. T., Gladman, B. J., Kavelaars, J. J., et al. 2018, *ApJS*, **236**, 18
 Bannister, M. T., Kavelaars, J. J., Petit, J.-M., et al. 2016, *AJ*, **152**, 70
 Beaudoin, M., Gladman, B., Huang, Y., et al. 2023, *PSJ*, **4**, 145
 Benecchi, S. D., & Sheppard, S. S. 2013, *AJ*, **145**, 124
 Bernstein, G. M., Trilling, D. E., Allen, R. L., et al. 2004, *AJ*, **128**, 1364
 Bianco, F. & The Rubin Observatory Survey Cadence Optimization Committee 2023, Survey Cadence Optimization Committee's Phase 2 Recommendations PSTN-055, Vera C. Rubin Observatory <https://pstn-055.lsst.io/>
 Bianco, F. & The Rubin Observatory Survey Cadence Optimization Committee 2024, Survey Cadence Optimization Committee's Phase 3 Recommendations PSTN-056, Vera C. Rubin Observatory <https://pstn-056.lsst.io/>
 Bianco, F. B., Jones, L., Željko, I., Steven, R., et al. 2022, Updated Estimates of the Rubin System Throughput and Expected LSST Image Depth PSTN-054, Vera C. Rubin Observatory <https://pstn-054.lsst.io/>
 Bonnarel, F., Fernique, P., Bienaymé, O., et al. 2000, *A&AS*, **143**, 33
 Buie, M. W., & Keller, J. M. 2016, *AJ*, **151**, 73
 Buie, M. W., Spencer, J. R., Porter, S. B., et al. 2024, *PSJ*, **5**, 196
 Cheng, A. F., Weaver, H. A., Conard, S. J., et al. 2008, *SSRv*, **140**, 189
 Chiang, E. I., & Brown, M. E. 1999, *AJ*, **118**, 1411
 Cromptovets, B. L., Lawler, S. M., Volk, K., et al. 2022, *PSJ*, **3**, 113
 da Costa-Luis, C., Larroque, S. K., Altendorf, K., et al. 2023, tqdm: A fast, Extensible Progress Bar for Python and CLI, v4.66.1, Zenodo, doi:10.5281/zenodo.8233425
 Desch, S., & Neveu, M. 2017, *Icar*, **287**, 175
 Doner, A., Horányi, M., Bagenal, F., et al. 2024, *ApJL*, **961**, L38
 Fraser, W. C., Porter, S. B., Benecchi, S. D., et al. 2024b, *LPSC*, **55**, 2440
 Fraser, W. C., Porter, S. B., Peltier, L., et al. 2024a, *PSJ*, **5**, 227
 Gladman, B., & Volk, K. 2021, *ARA&A*, **59**, 203
 G'orski, K. M., Hivon, E., Banday, A. J., et al. 2005, *ApJ*, **622**, 759
 Grundy, W. M., Bird, M. K., Britt, D. T., et al. 2020, *Sci*, **367**, aay3705
 Harris, C. R., Millman, K. J., van der Walt, S. J., et al. 2020, *Natur*, **585**, 357
 Holman, M. J., Akmal, A., Farnocchia, D., et al. 2023, *PSJ*, **4**, 69
 Holman, M. J., Bernardinelli, P. H., Schwamb, M. E., et al. 2025, *AJ*, **170**, 97
 Hunter, J. D. 2007, *CSE*, **9**, 90
 Jones, R. L., Slater, C. T., Moeyens, J., et al. 2018, *Icar*, **303**, 181
 Kavelaars, J., Lawler, S. M., Bannister, M. T., & Shankman, C. 2020, in The Trans-Neptunian Solar System, ed. D. Pralnik, M. A. Barucci, & L. A. Young (Amsterdam: Elsevier), 61
 Kavelaars, J. J., Petit, J.-M., Gladman, B., et al. 2021, *ApJL*, **920**, L28
 Kluyver, T., Ragan-Kelley, B., Pérez, F., et al. 2016, Positioning and Power in Academic Publishing: Players, Agents and Agendas (Amsterdam: IOS Press), 87
 Krasnopolsky, V. A. 2020, *Icar*, **335**, 113374
 Lam, S. K., Pitrou, A., & Seibert, S. 2015, in Proc. of the Second Workshop on the LLVM Compiler Infrastructure in HPC, ed. H. Finkel (New York: Association for Computing Machinery), 7
 Lawler, S. M., Kavelaars, J. J., Alexandersen, M., et al. 2018, *FrASS*, **5**, 14
 Lawler, S. M., & Pike, R. E. 2024, arXiv:2410.04338
 McKinney, W. 2010, Proc. 9th Python in Science Conf., ed. S. van der Walt & J. Millman, (SciPy), 56
 McKinnon, W. B., Richardson, D. C., Marohnic, J. C., et al. 2020, *Sci*, **367**, aay6620
 Mommert, M., Kelley, M., de Val-Borro, M., et al. 2019, *JOSS*, **4**, 1426
 Merritt, S. R., Fedorets, G., Schwamb, M. E., et al. 2025, *AJ*, **170**, 100
 Napier, K. 2024, TNO2024: The Trans-Neptunian Solar System, 4.10, <https://tno2024.org/relation/abstract/46>
 Napier, K. J., Lin, H.-W., Gerdes, D. W., et al. 2024, *PSJ*, **5**, 50
 Nesvorný, D., Bernardinelli, P., Vokrouhlický, D., & Batygin, K. 2023a, *Icar*, **406**, 115738
 Nesvorný, D., Dones, L., De Prá, M., Womack, M., & Zahnle, K. J. 2023b, *PSJ*, **4**, 139
 Nesvorný, D., Li, R., Simon, J. B., et al. 2021, *PSJ*, **2**, 27
 Nesvorný, D., Vokrouhlický, D., & Fraser, W. C. 2022, *AJ*, **163**, 137
 Peltier, L., Kavelaars, J., Fraser, W., et al. 2022, AAS/DPS Meeting, **54**, 501.09
 Petit, J.-M., Gladman, B., Kavelaars, J., et al. 2023a, AAS/DPS Meeting, **55**, 209.04
 Petit, J.-M., Gladman, B., Kavelaars, J. J., et al. 2023b, *ApJL*, **947**, L4
 Polak, B., & Klahr, H. 2023, *ApJ*, **943**, 125
 Porter, S., Singer, K. N., Schenk, P., et al. 2024, AGU Fall Meeting, **2024**, P24B
 Porter, S. B., Spencer, J. R., Benecchi, S., et al. 2016, *ApJL*, **828**, L15
 Rein, H., Holman, M., & Akmal, A. 2023, matthewholman/assist: v1.1.1, Zenodo, doi:10.5281/zenodo.7778017
 Rein, H., & Liu, S. F. 2012, *A&A*, **537**, A128
 Rein, H., & Spiegel, D. S. 2015, *MNRAS*, **446**, 1424
 Robbins, S. J., & Singer, K. N. 2021, *PSJ*, **2**, 192
 Robinson, J. E., Fraser, W. C., Fitzsimmons, A., & Lacerda, P. 2020, *A&A*, **643**, A55
 Singer, K. N., McKinnon, W. B., Gladman, B., et al. 2019, *Sci*, **363**, 955
 Skrutskie, M. F., Cutri, R. M., Stiening, R., et al. 2006, *AJ*, **131**, 1163
 Smotherman, H., Bernardinelli, P. H., Portillo, S. K. N., et al. 2024, *AJ*, **167**, 136
 Smotherman, H., Connolly, A. J., Kalmbach, J. B., et al. 2021, *AJ*, **162**, 245
 Stern, S. A., Bagenal, F., Ennico, K., et al. 2015, *Sci*, **350**, aad1815
 Stern, S. A., Weaver, H. A., Spencer, J. R., et al. 2019, *Sci*, **364**, aaw9771
 Stern, S. A., White, O. L., Grundy, W. M., et al. 2023, *PSJ*, **4**, 176
 Strauss, R., Trilling, D. E., Bernardinelli, P. H., et al. 2024, *AJ*, **167**, 135
 The pandas development team 2020, pandas-dev/pandas: Pandas, v2.3.1, Zenodo, doi:10.5281/zenodo.3509134
 Trilling, D. E., Bannister, M., Fuentes, C., et al. 2018, arXiv:1812.09705
 Uieda, L., Soler, S., Rampin, R., et al. 2020, *JOSS*, **5**, 1943
 Verbiscer, A. J., Helfenstein, P., Porter, S. B., et al. 2022, *PSJ*, **3**, 95
 Verbiscer, A. J., Porter, S., Benecchi, S. D., et al. 2019, *AJ*, **158**, 123
 Virtanen, P., Gommers, R., Oliphant, T. E., et al. 2020, *NatMe*, **17**, 261
 Weaver, H. A., Cheng, A. F., Morgan, F., et al. 2020, *PASP*, **132**, 035003
 Weaver, H. A., Porter, S. B., Spencer, J. R. & The New Horizons Science Team 2022, *PSJ*, **3**, 46
 Wong, M. L., Fan, S., Gao, P., et al. 2017, *Icar*, **287**, 110
 Yoachim, P., Jones, R. L., Neilsen, E. H., et al. 2022, lsst/rubin_sim: v0.12.1, Zenodo, doi:10.5281/zenodo.7087823
 Yoshida, F., Yanagisawa, T., Ito, T., et al. 2024, *PASJ*, **76**, 720
 Zonca, A., Singer, L., Lenz, D., et al. 2019, *JOSS*, **4**, 1298